



DOI: 10.5281/zenodo.1069527

# LUMINESCENCE DATING AND MINERALOGICAL INVESTIGATIONS OF BRICKS FROM ERIKLI BASILICA IN STRATONIKEIA ANCIENT CITY (SW-TURKEY)

Mehmet Altay Atlıhan<sup>1</sup>, Tamer Koralay<sup>2</sup> and Eren Sahiner<sup>3</sup>

<sup>1</sup>*Pamukkale University, Faculty of Science and Letters, Department of Physics, Kınıklı Campus 20017 Denizli, Turkey*

<sup>2</sup>*Pamukkale University, Faculty of Engineering, Department of Geological Engineering, Kınıklı Campus 20017 Denizli, Turkey*

<sup>3</sup>*Ankara University, Institute of Nuclear Sciences, Beşevler Campus 06100 Ankara, Turkey*

Received: 24/11/2017

Accepted: 25/01/2018

Corresponding author: Mehmet Altay Atlıhan (aatlihan@pau.edu.tr)

## ABSTRACT

Stratonikeia is one of the oldest settlements in southwestern Anatolia and at the same time significant for an understanding of the Hellenistic period. Archaeological records of Stratonikeia date back to around 2000 BC. This study provides new information not only about luminescence age but also about mineralo-petrographic, geochemical characteristics of bricks taken from Erikli Basilica in Stratonikeia (Turkey). In this study, mineralogical data of TL and OSL dating of two bricks and two sediment samples will be presented. The bricks have highly similar mineralogical composition, consisting mainly of quartz and muscovite. These results are supported by XRD studies. In order to perform the thermoluminescence (TL) and optically stimulated luminescence (OSL) dating, the equivalent dose (ED) and the annual dose (AD) of the samples were determined using different estimation techniques. The TL ages of bricks are determined to be  $1189 \pm 89$  and  $576 \pm 40$  years. The IRSL ages of the bricks are determined to be  $1167 \pm 85$  years and  $545 \pm 50$  years. Additionally, supporting the TL and IRSL ages, the OSL quartz ages of the two sediments obtained from the top of the layer under the floor are discovered to be about 1100 years. Mineralo-petrographic, geochemical, dating and archaeological studies have revealed that the age of bricks is different from each other. Furthermore, Erikli Basilica was built in bricks, consisting of raw materials taken from different quarries in different periods. Within the framework, the first report of the experimental approach has been published from Stratonikeia archaeological site located in Muğla, Aegean Anatolia.

---

**KEYWORDS:** Luminescence spectroscopy, Dating, Mineralogy, XRF and XRD, Ancient bricks

---

## 1. INTRODUCTION

Stratonikeia, a city in the interior of Caria, is located at Eskihisar village within the borders of Yatağan town of Muğla province (Fig. 1). Stratonikeia has been named after the wife of I. Antiokhos, who is one of the Emperor of Seleukos, and it has been known as the city of gladiators and eternal love (<http://stratonikeia.pau.edu.tr>, 2017). Muğla province is the archaeologically richest and the most significant region in SW Turkey today. Since Muğla has a strategic location, being the passageway between the inner Aegean and the eastern Mediterranean regions, it has hosted many ancient settlements in dif-

ferent time periods. The first scientific excavation at the site began in 1977. The Stratonikeia settlement was named by pre-historians as “Chrysaoris or Idrias”. After 281 B.C., the Seleucid King Antiochos I, changed the name of the city to Stratonikeia (Hanfmann and Waldbaum, 1968; <http://stratonikeia.pau.edu.tr>, 2017). Stratonikeia and the surrounding region changed hands among the Seleucids, the Ptolemaics, the Macedonians, Rhodians and Romans. This ancient city passed under Turkish control in 12<sup>th</sup> century AD. (Sögüt and Yılmaz, 2012).



Figure 1. Location map of the Stratonikeia antique city.

In ancient times, bricks were used as a building material. Hence, studies regarding these materials are crucial to understanding ancient societies. Dating studies, mineralo-petrographic, geochemical and provenance analyses of bricks have great importance for archaeological studies, restoration works. Some geological analyses (e.g. FTIR, XRD, SEM-EDX) were used to characterize the mineralogical structures of pigments of some samples from this site (Bahçeli et al., 2016). Moreover, chemical and mineralogical analysis of various pottery sherd samples have been recently analyzed by Javanshah (2018) using different techniques such as X-ray Fluorescence (XRF) and Scanning Electron Microscopy (SEM) with Energy Dispersive X-ray Spectroscopy (EDS). Optically stimulated luminescence (OSL) and thermoluminescence (TL) dating techniques have been commonly

applied for getting the chronological information of archaeological sites (Aitken, 1985; Öke and Yurdatapın, 2000; Liritzis et al., 2010; Aitken, 2013; Bortolussi et al., 2013; Şahiner et al. 2013; Doğan and Meriç, 2014; Liritzis et al. 2013b; Liritzis and Vafiadou, 2015). The luminescence is a measuring process of the light resulting from the recombination of electrons and holes from metastable trapping states at crystal defects. Energy derived mainly from radioactive minerals (e.g. U, Th, K, Rb) in sediments yields storage of electrons at traps. When a sample is stimulated by heating (in TL) or light (in OSL), electrons and holes are ejected and then recombined with carriers of opposite charges. Luminescence is finally emitted from the sample. Depending on the wavelength used for stimulation light, the resulting luminescence is called either blue light stimulated

luminescence (BLSL; commonly known as OSL) or infrared light stimulated luminescence (IRSL). Different wavelengths of light are selected according to the contents of materials to be used in luminescence studies. For instance, blue light is used for quartz which is frequently employed throughout retrospective luminescence dosimetry researches (McKeever, 2011; Aitken, 1985; Correcher and Delgado, 1998). Additionally, using IR stimulation at various temperatures as well as a combination of IR and blue stimulations could be considerably effective in the case of feldspathic minerals, polymineral and contaminated quartz samples regarding dating applications (Thomsen et al., 2008; Ankjærgaard et al. 2010; Li, 2010; Şahiner et al. 2014a, 2017a, 2017b).

The measurements of equivalent dose and annual dose rate are required for dating. The dose absorbed by the buried sample, called also as equivalent dose (ED or  $D_e$ ), is obtained by comparing the natural luminescence signal with signals originated from different amounts of laboratory doses. Two main protocols have been advanced for the assessment of equivalent dose. The protocols are Multiple Aliquot Additive Dose (MAAD) and Single Aliquot Regeneration (SAR). These protocols can be appealed for the details of these procedures (Aitken, 1985). The dose absorbed by the buried sample for one year is referred to as the annual dose or annual dose rate (AD or  $D_a$ ). The concentration of radioactive minerals in the sample, the magnitude of the contribution of cosmic rays and environmental conditions need to be known to find the annual dose rate. The age is determined by dividing the value of the equivalent dose by the annual dose rate.

The present study aims to provide the first luminescence dating data on bricks of Erikli Basilica in the archaeological site. In this basilica, mosaic ornaments that are not common in the region were observed. Archaeological evidence has proven that basilica was used from the late 5<sup>th</sup> century until the beginning of the 7<sup>th</sup> century A.D. A total of 71 coins were found within the building. 36 of the coins were dated back to the Byzantine period, ranging from the reign of Iustinianus I. (527-565) to that of Heraclius (610-641). The remaining 34 coins could not be identified. However, one piece could be attributed to the Emperor Constantinos VII. (913-959). Archaeologists are interested in whether this piece from the 10<sup>th</sup> century indicates the last date of usage of the basilica (<http://stratonikeia.pau.edu.tr>, 2017). This should be confirmed or disconfirmed by dating of some samples which could be taken from the floor of the building. So, a floor tile (first brick sample: STRN-1) was taken from the basilica. This tile is from the top layer of the bottom of the basilica which became available after the excavations. Thus, its age indi-

cates the latest date when the building was used as a basilica. In addition, sediment samples were taken from the top of the layer under the floor tile and another adjacent floor tile (STRN-2 and STRN-3). These samples indicate the date on which the floor tiles were placed. From this date on, exposure of sediment samples to daylight has been blocked. Our assumption is that the ages of these samples are more or less similar.

It is also a matter of curiosity whether the building was used with different purposes with a few simple renovations after it had been used as a basilica. In order to shed light on this issue, a piece of brick (second brick sample: STRN-4) from the western wall of the ruins, which might belong to the later periods, was selected. If there is a significant time period between the production dates of these bricks samples (STRN-1, STRN-4), we believe that their materials might be collected from the sand quarries in different regions. If so, the chemical and mineralogical contents of the samples must be different from each other. In order to define any differences between the bricks, mineralo-petrographic investigations are performed on the same samples.

## 2. EXPERIMENTAL PROCEDURES FOR MINERO-PETROGRAPHIC INVESTIGATIONS

To determine the differences between the bricks, specific analytical procedures were performed on samples. Firstly, to define mineral compositions of the bricks, the following steps and analyses were followed: **i)** mineralogic parameters (i.e. mineral association, grain size and structure, voids properties of bricks) were examined under polarized light microscope using thin sections; **ii)** qualitative mineralogical composition of the brick samples was determined with X-ray Diffraction (XRD), using Inel Equinox 1000 diffractometer (Instrumental condition: Co-K $\alpha$  radiation obtained at 30 kV and 30 Ma, 0-100° 2 $\theta$  investigated range, 0.030° step) in the Earth Science Application & Research Center of Ankara University (YEBİM). In this study, two bricks samples were analyzed. The analyzed samples were finely grounded by tungsten carbide crushing vessel. Then a few milligrams of the powder were placed on sample holder and put into the XRD set-up.

Major oxide and trace elements for the samples were analyzed by a Spectro XEPOS Polarized Energy Dispersive X-ray Fluorescence (PED-XRF) spectrometer at the Department of Geological Engineering at Pamukkale University. The SPECTRO XEPOS uses a 50 W Pd end window X-ray tube. The spectral resolution of this detector is 160 eV for Mn K $\alpha$ . During the measurement, the sample chamber is flushed with He. For the XEPOS XRF analyses, two brick

samples were crushed in a tungsten carbide crushing vessel, and 6.25 g of powdered sample was mixed with 1.4 g of wax. The mixture was pressed at 20 N in an automatic press to obtain a pressed disc (Kadioğlu *et al.*, 2009; Koralay and Kılınçarslan, 2016; Güllü and Kadioğlu, 2017).

### 3. APPLIED ANALYTICAL PROCEDURES FOR LUMINESCENCE DATING

Luminescence dating was carried out by using OSL, IRSL and TL techniques for brick samples. To obtain the ED, IRSL MAAD and IRSL/OSL SAR protocols are used. Similarly, only MAAD protocol was applied in TL. In these applications, polymineral materials obtained from the brick samples are used. However, it was observed that there is plenty of quartz in the sediment samples. For this reason, the age of sediment samples was determined by OSL technique using quartz particles obtained from these samples. Thus, it was also possible to compare the ages determined by using different techniques.

An Optical Dating System, model ELSEC-9010, was used for IRSL measurements. In case of IRSL, polymineral samples were optically stimulated using infrared light emitted by a diode array (wavelength  $880\pm 80$  nm); a filter and Schott BG 39. The measured signal is called infrared stimulated luminescence (IRSL). The ELSEC system is equipped with a  $^{90}\text{Sr}/^{90}\text{Y}$  beta radiation source, with nominal dose rate of 0.027 Gy/s.

All quartz OSL measurements were performed with a Risø TL/OSL reader (TL/OSL-DA-20, Risø) equipped with a  $^{90}\text{Sr}/^{90}\text{Y}$  beta particle source, delivering a nominal dose rate of  $0.130 \pm 0.004$  Gy/s, a 9635QA photomultiplier tube and 7.5 mm Hoya U-340 filter. The stimulation wavelength is  $470\pm 20$  nm for the case of blue stimulation (OSL), delivering at the sample position a maximum power of 40 mW/cm<sup>2</sup>.

TL measurements were performed using a Harshaw 3500 reader system. A standard clear glass filter was always installed in the reader between the planchet and the photomultiplier tube. All measurements were carried out under pure nitrogen gas conditions to avoid undesired signal and temperature lags.

The assessment of the annual dose for the sample was accomplished by evaluating the specific activities of main radionuclides (U, Th, and  $^{40}\text{K}$ ) contained in the sample, through gamma spectrometry (coaxial-type HPGe detector, ORTEC Ltd.). For detector measurements, the samples were firstly utterly dried at 110 °C for 6 hours and then reduced to  $<500$  µm by crushing and sieving. Then, soil from the surroundings of the samples was put in cylindrical plastic boxes having the even geometry with those used

in the calibration shape. The gamma spectrometry system was calibrated with both energy and efficiency calibration using certificated point sources and reference materials, correspondingly. All related details about the calibrations, activity determinations, dose rate calculations, and correction factors of used HPGe system were presented by Şahiner & Meriç (2014) and Şahiner (2015). The detector measurements to determine radionuclide concentrations were performed after radioactive balance ensued (at least 5 weeks) in the isolated plastic boxes. Then, the dose rate was calculated based on the decay of naturally occurring radionuclides inside the clay matrix, i.e.,  $^{232}\text{Th}$ ,  $^{40}\text{K}$ , and natural U, along with cosmic rays theoretically obtained from geographical location. Internal dose rates were also taken into account in all samples, as shown in Table 2. The effects of the saturation water content (W factor in Table 2) were determined by commercial moisture analyzer. The dose conversion factors were calculated by using both Adamiec and Aitken (1998) and Liritzis *et al.*'s (2013a) studies.

All pre-handling and luminescence measurements were performed under subdued red-light conditions. For IRSL and TL measurements: The outer surface (3 mm) of brick samples were discarded to eliminate the part exposed to sunlight. The rests were crushed gently until it became powder. They were washed, respectively, with 10% HCl and 35% H<sub>2</sub>O<sub>2</sub> to remove carbonates and organic materials. Afterwards they were washed in distilled water and then were dried and sieved to obtain the size of polymineral fine grains ( $<20$ µm). Afterwards, the grains were deposited in a thin layer with silicon spray on the aluminum discs of 10 mm diameter and 0.5 mm thickness. These prepared discs are called aliquots. Thus, these aliquots turned out to be ready for measurements. To eliminate the influence of the unstable traps on luminescence counts, which are performed to find out the equivalent dose (ED), discs are preheated before ED measurements. A procedure for the determination of preheating temperature and duration can be found in literature (Aitken, 1985). After the measurements, it was found that 200 °C and 12 min were suitable for the sample. Anomalous fading losses were neglected because of relatively young ages of bricks but they have been considered while calculating uncertainties.

For quartz OSL measurements: Samples were sieved as grains of dimensions 90-140 µm were obtained, which were treated with HCl (10%), H<sub>2</sub>O<sub>2</sub> (35%), to remove carbonate and organic material, respectively. Then, to separate quartz from feldspar and heavy-minerals, a density liquid is used. Ultimately, quartz samples were etched with HF (40%, 45-60 min of handling) and a final treatment with

HCl (10%) in order to obtain a clean mineral. After every step of chemical treatment, the sample is fully washed with pure water. Aliquots with mass of 2 mg each were prepared by mounting the material on disks. Absence of feldspars were checked with infrared (IR) stimulation at ambient temperature from at least 3 aliquots. There is no contribution of feldspars signal (lower than %1 of quartz) observed in the quartz samples.

### 3.1. Equivalent dose (ED) measurements

In order to determine Equivalent Dose, MAAD and SAR procedures were used in IRSL technique and solely MAAD procedure was used in TL technique. Here, irradiated aliquots were left for 24 h and were subjected to preheating before applying normalization and luminescence measurements. Also, each luminescence count was made in 160 s in IRSL. Within the SAR procedures, disks were subjected to bleaching under sunlight until all residual signals were erased.

#### 3.1.1. MAAD procedure - IRSL

(IRSL: polymineral grains taken from STRN1 and STRN4)

Aliquots were divided into four groups, each one including four aliquots. While one group was not irradiated (no additive dose) for natural dose, the others were irradiated with different additive doses (2, 5, 10 Gy). Luminescence measurements were performed and the mean values from each group were plotted against additive dose. Sixteen aliquots were used in this procedure. Normalization was carried out after the luminescence measurement.

#### 3.1.2. SAR procedure - IRSL/OSL

(IRSL: polymineral grains taken from STRN-1 and STRN-4, OSL: quartz grains taken from STRN-2 and STRN-3)

*In IRSL:* At first, luminescence signal obtained from a single aliquot was measured to determine the beginning signal. The signal point was associated with equivalent dose. Then, the aliquot was bleached. Secondly, it was given a regenerative dose and luminescence read again. Bleach, irradiation and measurement procedures were repeated for 2, 4, 8 and 12 Gy doses. The build-up curve for this aliquot was plotted against the laboratory dose-luminescence signal and then the ED was calculated. This procedure was applied to six aliquots. So, the determination of equivalent dose through this experiment was repeated six times independently. Moreover, Monte Carlo simulations, based on a stochastic sampling of luminescence intensity, were estimated for interpolation points, approaching to estimate the uncertainty in the ED value. The paper by Duller (2007) details describes comparisons of approximations with numerous example data sets on equivalent dose estimates of single aliquot regenerative dose measurements.

*In OSL:* As illustrated in Table 1, Improved-Single Aliquot Regenerative Dose (SAR) Protocol was used so as to calculate equivalent dose developed by Murray et al. (1998) for quartz samples. For this purpose,  $D_i$  is elevated doses until nearly 60 Gy and determined test dose ( $D_t$ ) is 1 Gy obtained from previous IR check step. And, ages were determined from fast component of quartz as well as using 16 aliquots to Central Age Model (CAM) which have <20% scattering ratio.

Table 1. Applied SAR protocol to quartz samples

Step	Treatment	Observed
1	Dose, $D_i$	
2	Preheat , 220°C, 2°C/s, 10 s	
3	OSL, 200s at 110°C, 2 °C/s	$L_i$
5	Test dose, $D_t$	
6	Preheat , 220°C, 2°C/s, 10s	
7	OSL, 200s at 110°C, 2°C/s	$T_i$
8	Return to step 1	

#### 3.1.3. MAAD procedure - TL

Linear heating was used for stimulation in TL technique. All TL measurements were carried out by using a heating rate of 2 °C/s up to a maximum temperature of 500 °C. The equivalent dose was found by collecting the TL curves between 280 °C and 350°C, derived from plateau test (Aitken 1985).

The steps in MAAD procedure of IRSL were repeated here, too.

### 3.2. Dose rate (annual dose) measurements

Components of annual dose rate are given in Table 2. The dose rates of the ionizing radiations were defined by detecting densities of the main radioactive isotopes of the uranium and thorium series and

the potassium at a high-purity germanium detector (coaxial-type HPGe detector, ORTEC Ltd.). Since the water content of the sample plays an important role in the absorption of the radiation from minerals, saturation water content measurements were performed via humidity analyzer. The annual cosmic-ray contribution was calculated from the geographical location of Stratonikeia and environmental conditions following Prescott and Hutton (1994). The water uptake during burial, F factor, ( $0.6\pm 0.2$ ) was presumed, as in Aitken (1985). Thus, annual doses were calculated using conversion factors asserted by Adamiec and Aitken (1998) and its updated version by Liritzis *et al.* (2013a). The annual dose rate and luminescence age calculation were comparatively carried out by using online calculator published by

Durcan *et al.* (2015) and a user-friendly java application released by Tsakalos *et al.* (2016). These software programs are user-friendly and they can consider all details of luminescence dating multiple variables and the propagation of uncertainties. Moreover, calculated attenuation factors for both alpha and beta were presented in Table 2. Due to the fact that attenuation factors depend on grain sizes and radionuclide types, calculations were conducted by mean transmission factor of each radioisotopes in samples. As for the variation of the gamma dose-rate contribution on bricks, it was taken from Aitken (1985), with correction for the average density. Similar approximations were performed by Polymeris and Kitis (2011).

*Table 2. Results of annual dose components with concentration of radionuclides in samples.*

Sample Codes	U (ppm)	Th (ppm)	K (%)	Alpha attenuation factor, a	Beta attenuation factor, b	ACD (mGy/a)	W	Internal Dose (mGy/a)	Annual Dose (mGy/a)
STRN-1	6.12±0.21	14.24±0.43	2.37±0.07	0.467	0.947	0.15±0.02	0.38±0.04	1.441±0.334	5.93±0.18
STRN-2	4.90±0.09	10.89±0.08	1.61±0.06	0.006	0.760	0.32±0.02	0.25±0.05	0.097±0.021	3.52±0.12
STRN-3	5.71±0.09	10.59±0.08	1.57±0.05	0.006	0.760	0.32±0.02	0.22±0.05	0.098±0.020	3.95±0.13
STRN-4	6.67±0.23	17.07±0.51	2.22±0.06	0.461	0.942	0.15±0.02	0.52±0.05	1.619±0.371	5.83±0.14

#### 4. MINERALOGICAL COMPOSITION OF BRICKS

Bricks are mostly composed of clay-rich inorganic materials that have been widely used in ancient times. Many functional objects including small goods (such as bibelot, mosaic tables, vases of various form, bowls and dishes, drug jars) and greater objects (brick, paving stone) which are made from ceramics, have been documented in many archaeological excavations. The detailed investigations on the ancient brick/ceramic materials are called as "Ceramic Compositional Analysis" (Reedy, 2008; Quinn, 2013). A number of papers have been published to define the scientific characteristics of ceramics (Cardiano *et al.*, 2004; Hill *et al.*, 2004; Belfiore *et al.*, 2007; Velosa *et al.*, 2007; Morra *et al.*, 2013). The characterization of bricks provides helpful information for answering some questions about the production and function of bricks.

According to the macroscopic properties (color, grain size and void proportions), the bricks can be separated from each other. STRN-1 sample shows uniformly orange color and has very small grain size in hand specimen. STRN-4 sample is light brown in color and contains fine-grained lithic fragments (rock and reworked ceramics). Lithic fragments are visible to naked eye or can be seen through a simple hand lens (Fig. 2a, b).

The detailed thin section and XRD properties of bricks are given below. STRN-1 consists of quartz and micas (muscovite and lesser amount of biotite); feldspar (orthoclase, rarely plagioclase) also exists within mineral composition. It is a well-sorted brick that has a modal grain size of 0.04–0.23 mm for quartz grain, 0.12–0.35 mm for mica grains. Furthermore, there is a negligible amount of quartzite and reworked brick fragments in STRN-1 sample (Fig. 2c, d).

STRN-4 contains similar mineral types with STRN-1. Quartz and mica minerals are the prevalent components of the brick. Quartz grains usually have angular shape and their sizes range between 0.12 and 0.34 mm. Micas are in the form of thin-long, needle-shaped grains. They vary in size from less than 0.12 to over 0.29 mm in length (Fig. 2e, f). In addition, lithic fragments are spherical, ellipsoidal and angular in shape and they range from 0.6 to 1.5 mm in length. They are mostly composed of metamorphic rocks and reworked brick fragments. Metamorphic rocks comprise of quartzite/quartz schist and mica schist. These mineral compositions of the brick samples are consistent with the geological structure of the ancient city of Stratonikeia and its surroundings.

The brick samples show similar XRD patterns (Fig. 3). The XRD analysis indicates quartz and muscovite minerals as the dominant constituents of all samples. In addition, muscovite peaks are observed as more

significant in STRN-4 brick. The mineral compositions of bricks are quite similar. The main differences between STRN-1 and STRN-4 are the grain size and the proportion of minerals. The grain size and portion of STRN-4 are higher than they are in STRN-1 brick. This result is also supported by XRD studies.

The firing temperatures of the bricks can be estimated by their colors and mineralogic compositions. Varying colors from orange to light brown indicate that the firing temperatures of bricks were higher

temperature treatments (Quinn, 2013). Furthermore, mullite, cristoballite and hematite minerals that are high temperature products are not determined in the petrographic and XRD analysis. In this case, it can be suggested that the brick cooking temperature does not exceed approximately 800 °C (Quinn, 2013). Further works are required to examine this hypothesis such as using thermoluminescence techniques or thermo-FTIR spectroscopy analyses.

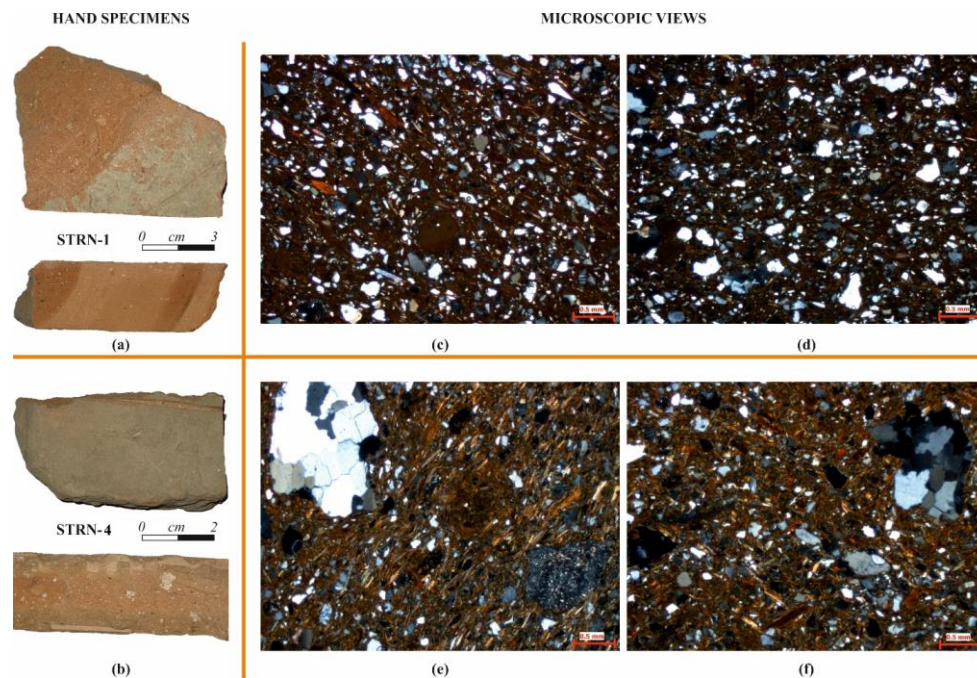


Figure 2 Hand specimens and their microphotographs of brick samples a) hand specimen of STRN-1 brick, b) hand specimen of STRN-4 brick, c, d) microphotographs of STRN-1, e, f) microphotographs of STRN-

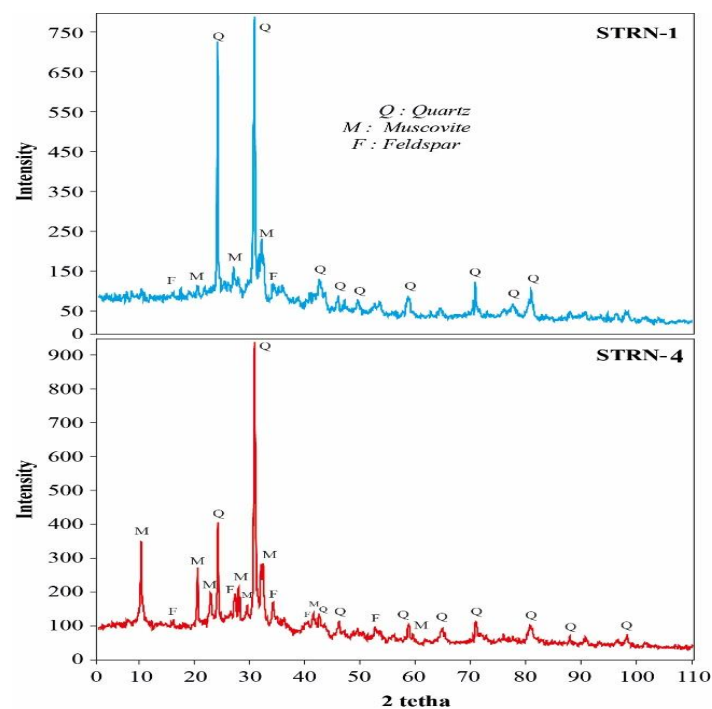


Figure 3 XRD analyzes of brick samples

## 5. CHEMICAL CHARACTERISTICS OF THE BRICKS

Major and trace element analyses have been carried out in order to identify the geochemical characteristics of the bricks. The results of the geochemical analysis of the brick samples are given in Table 3 and shown in the Fig. 4. According to these results, the bricks contain high amounts of  $\text{Fe}_2\text{O}_3$ ,  $\text{K}_2\text{O}$ ,  $\text{Al}_2\text{O}_3$ ,  $\text{SiO}_2$ , Rb and Zr and low amounts of MgO, CaO,  $\text{TiO}_2$ ,  $\text{Na}_2\text{O}$ , Co and Cu (Fig. 4). Furthermore, the STRN-4 brick has higher values than STRN-1 brick in terms of the MgO,  $\text{Fe}_2\text{O}_3$ , CaO, MnO,  $\text{P}_2\text{O}_5$ ,  $\text{SO}_3$ , Cl, Ce, Pr, Er, Ni and Zn elements. Additionally, the brick samples are notably similar to each other in

terms of  $\text{TiO}_2$ ,  $\text{Al}_2\text{O}_3$ , Co, Cu and Y elements. High K and low Ca contents in brick compositions suggest that local raw material sources (e.g. stream bed and colluvium) containing K-rich clay may have been used in the construction of bricks. Differences observed in the chemical composition of bricks can be related to their mineralogical compositions. In this case, two different interpretations could be made: **i)** bricks were prepared using raw materials from different sources in the same period. **ii)** bricks were made using raw materials from different sources in different periods. The second interpretation seems more acceptable because it is supported by TL and OSL dating studies.

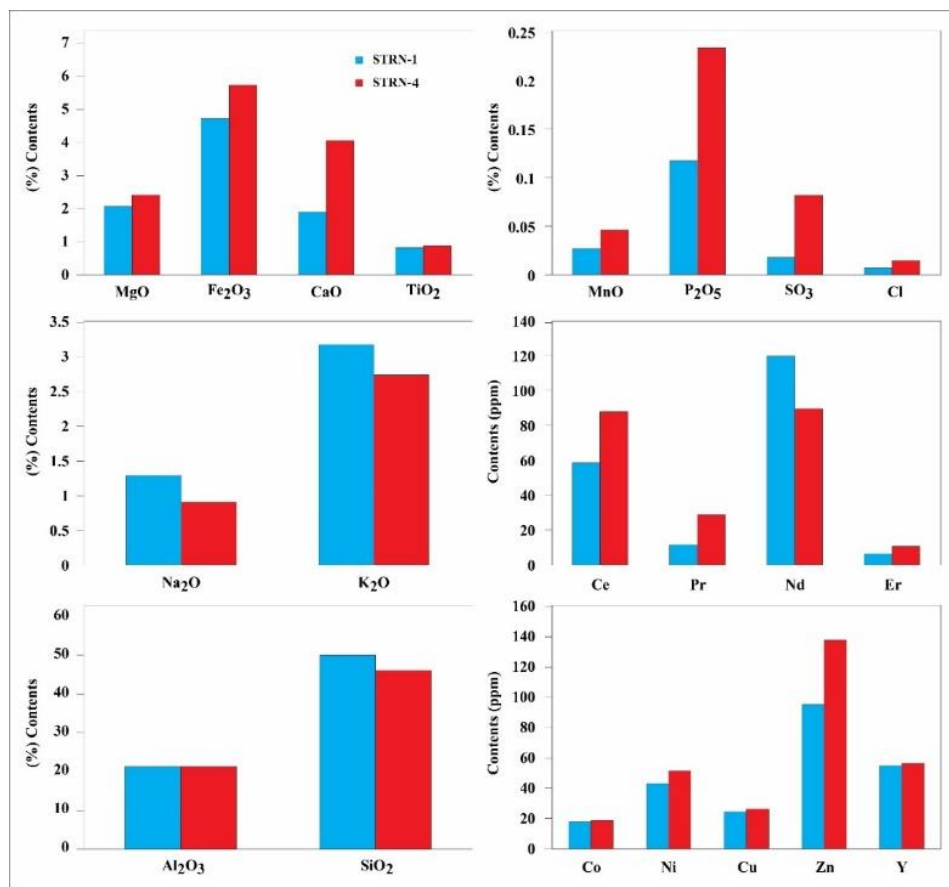


Figure 4 Major oxides and selected trace elements in brick samples

Table 3. Major oxide (%) and some trace elements (ppm) (REE) analyses of the brick samples

Elements	STRN-1	STRN-4	Elements	STRN-1	STRN-4	Elements	STRN-1	STRN-4
$\text{Na}_2\text{O}$ (%)	1,28	0,9	V (ppm)	101,8	93,2	Sr (ppm)	102	95,3
MgO (%)	2,07	2,41	Cr (ppm)	96,4	98,4	Y (ppm)	55,1	56,6
$\text{Al}_2\text{O}_3$ (%)	21,34	21,33	Co (ppm)	18,2	19	Zr (ppm)	235,8	237,5
$\text{SiO}_2$ (%)	50,22	46,26	Ni (ppm)	43,4	51,7	Nb (ppm)	17	17,5
$\text{P}_2\text{O}_5$ (%)	0,12	0,23	Cu (ppm)	24,8	26,6	Sn (ppm)	23,2	24,6
$\text{SO}_3$ (%)	0,02	0,08	Zn (ppm)	95,4	137,7	Ce (ppm)	58,6	88
$\text{K}_2\text{O}$ (%)	3,16	2,73	Ga (ppm)	30,8	31,4	Pr (ppm)	11,7	28,9
CaO (%)	1,89	4,05	Ge (ppm)	1,2	0,7	Nd (ppm)	119,9	89,7
$\text{TiO}_2$ (%)	0,82	0,87	As (ppm)	4,2	5,9	Er (ppm)	6,5	10,7
MnO (%)	0,03	0,05	Se (ppm)	0,8	0,6	Pb (ppm)	28,3	27,5
$\text{Fe}_2\text{O}_3$ (%)	4,72	5,72	Rb (ppm)	146,5	137,3			



## 6. RESULTS OF LUMINESCENCE DATING STUDIES

A typical IRSL decay curves and TL glow curves obtained from sample STRN-1 are shown in Fig. 5(a)

and 5(b), respectively. These figures show a natural IRSL or TL signals, along with artificial curves taken from aliquots irradiated with different additive doses.

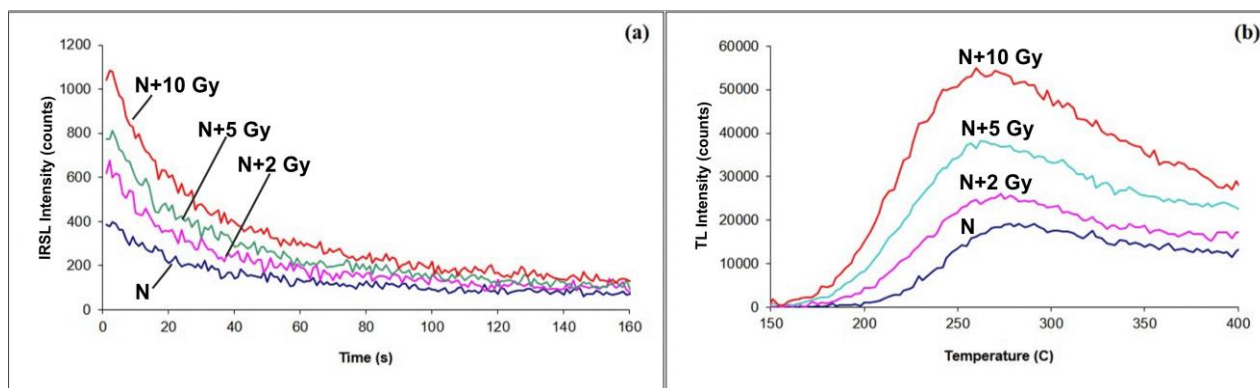


Figure 5 Additive dose procedure of STRN-1, namely the natural luminescence signal (N) along with three additive doses (2, 5, 10 Gy) a) IRSL decay curves b) TL glow curves

In order to determine the equivalent dose, MAAD procedure was applied in TL and IRSL, and the graphs of additive dose versus luminescence intensity are illustrated in Fig. 6a and in Fig. 6c for STRN-1 sample, respectively. Subtracting the background signal, the integral of entire IRSL signals were employed throughout estimations. Furthermore, equivalent dose plateau analysis is shown in Fig. 6b for temperatures between 250°C and 350°C using 1°C channel intervals. Intersection of extrapolation of the graph with horizontal axis gives the equivalent dose and supra-linearity correction (I) is estimated to be zero. Correspondingly, the equivalent dose is found through TL and IRSL to be  $7.04 \pm 0.28$  Gy and  $6.91 \pm 0.24$  Gy for STRN-1,  $3.36 \pm 0.04$  Gy and  $3.18 \pm 0.20$  Gy for STRN-4, respectively.

The equivalent dose values were determined by statistical distribution of doses from six aliquots. The graphs are shown in Fig. 7 only for STRN-1, because the graphs of the other sample are similar to those of STRN-1. The method interpolates the natural IRSL signal onto a growth curve. Fig. 7a indicates dose response with regular linear fitting and Fig. 7b denotes repeated dose calculation using Monte Carlo

simulation via *Analyst.exe* software for evaluation of luminescence dating results developed by Duller (2015) for Risø TL/OSL reader systems. On the other hand, sixteen aliquots of each sediment sample (STRN-2, STRN-3) were measured, and then the average value was worked out for improved SAR procedure that enabled to take sensitization changes into account at every regenerated dose cycle. In Fig. 8, a graphics of study is shown for one of the aliquots. Applied improved SAR protocol is exemplified in Table 1. While dots indicate experimental values, straight line shows exponential fitting results in Fig. 8a. Fig. 8b indicates that Monte Carlo simulation analyses of determined dose enable statically better results. Fig. 8c indicates sensitization changing over the SAR cycle owing to applied test dose, varying from about 0.8 to 1.3. Radial distribution of doses was demonstrated in Fig. 8d, yielding  $4.208 \pm 0.164$  Gy. The mean value of equivalent doses of the samples were determined to be  $4.51 \pm 0.12$  Gy (IRSL-SAR, STRN-1),  $4.21 \pm 0.16$  Gy (OSL-SAR, STRN-2),  $4.40 \pm 0.18$  Gy (OSL-SAR, STRN-2),  $2.17 \pm 0.09$  Gy (IRSL-SAR, STRN-4) and summary of these results are presented in Table 4.

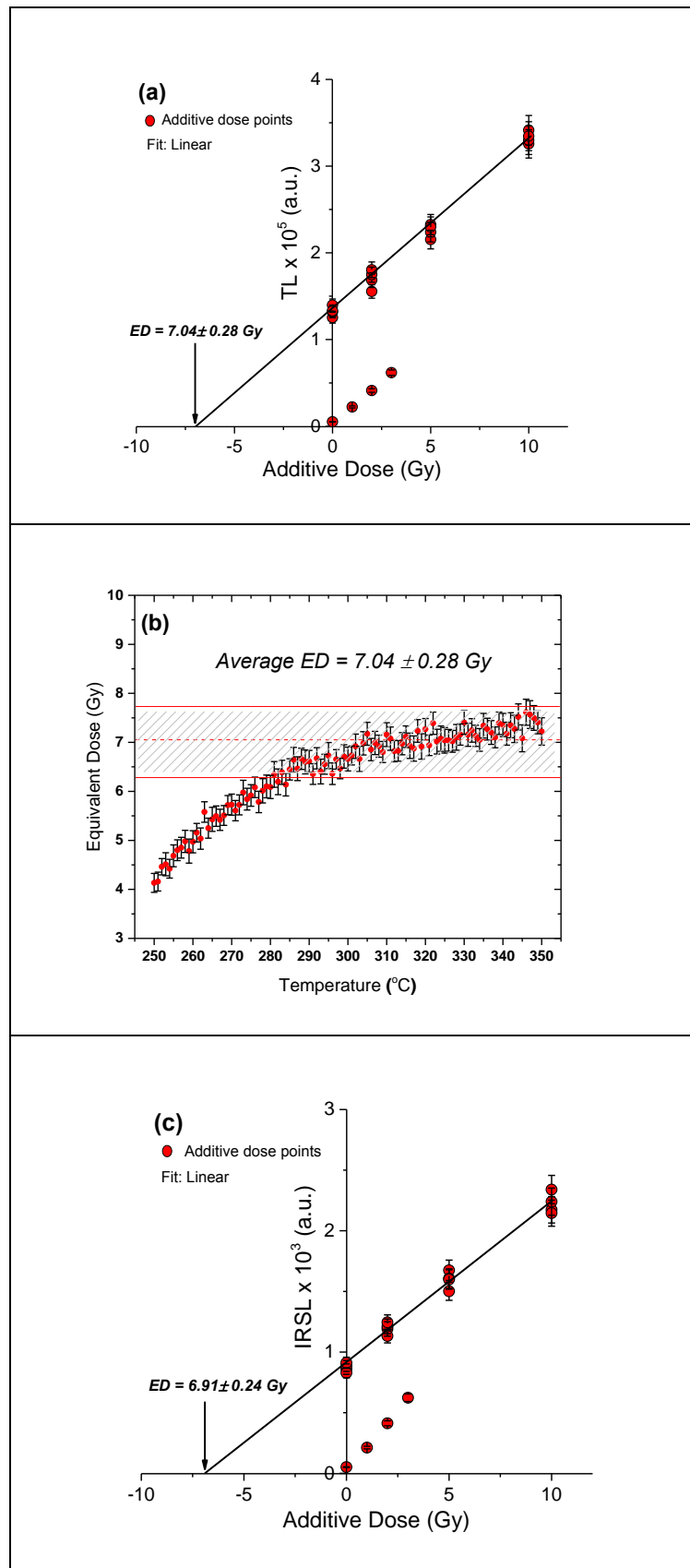


Figure 6 Applied MAAD procedure for STRN-1 sample: the same comparative ED analyses were done for both samples. The intercept of the extrapolated line on the horizontal axis gives the EDs. The arrows indicate the ED values; supra-linearity correction (I) is determined to be zero a) MAAD-TL dose response with linear fitting (b) Plateau test of ED between 250°C and 350°C temperatures (c) MAAD-IRSL dose response with linear fitting (whole integral of IRSL signals were taken into account for estimations)

Table 4. Determined equivalent doses and ages of the samples

Sample Codes	Methods	ED (Gy)	AD (mGy/a)	Age (a)
STRN-1	TL-MAAD procedure	7.04±0.28	5.93±0.18	1189±89
	IRSL-MAAD procedure	6.91±0.24		1167±85
	IRSL-SAR procedure	4.51±0.15		761±49
STRN-2	OSL-SAR procedure	4.21±0.16	3.52±0.12	1093±80
STRN-3	OSL-SAR procedure	4.40±0.18	3.95±0.13	1113±70
STRN-4	TL-MAAD procedure	3.36±0.04	5.83±0.14	576±40
	IRSL-MAAD procedure	3.18±0.20		545±50
	IRSL-SAR procedure	2.17±0.09		372±40

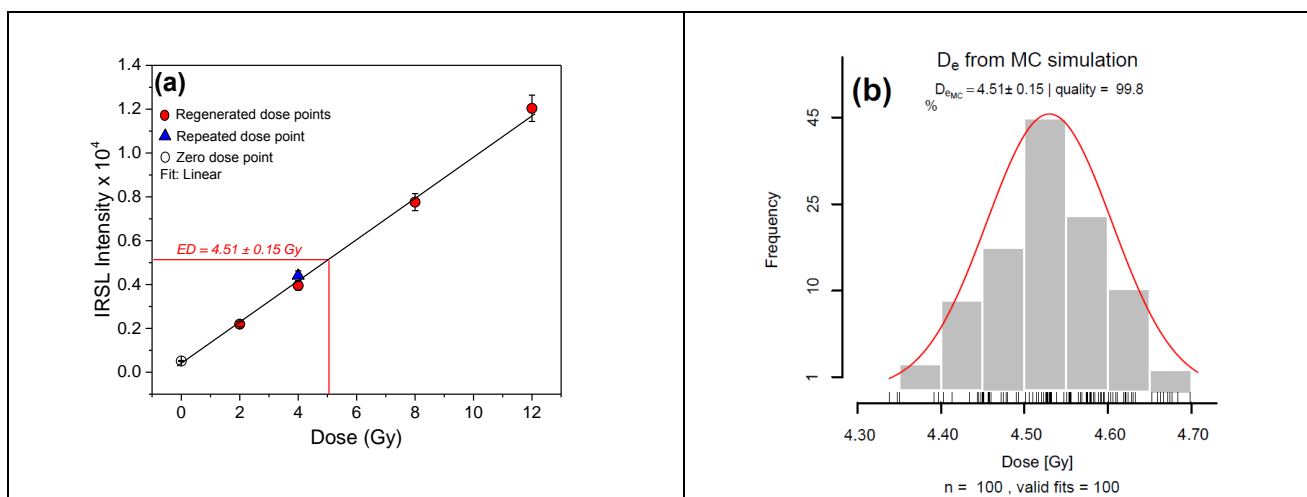
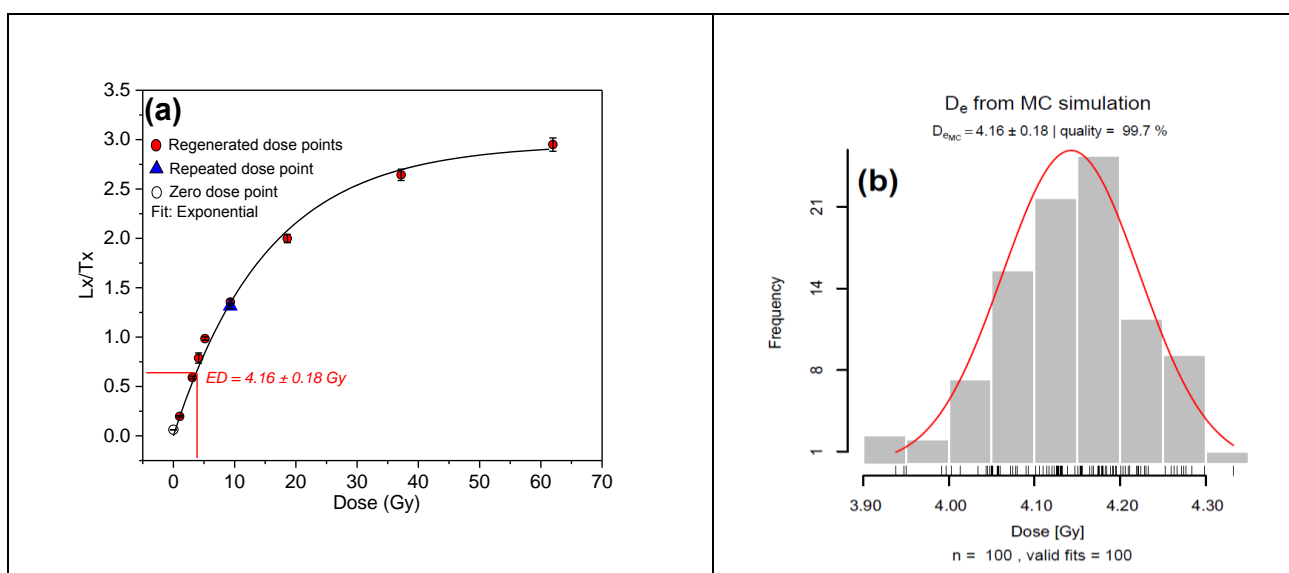


Figure 7 Regenerative dose response IRSL growth curves using the single aliquot method for STRN-1 to obtain the ED determination (a) dose response with linear fitting (b) Monte Carlo simulation analyses of estimated ED point, obtained from Analyst.exe software



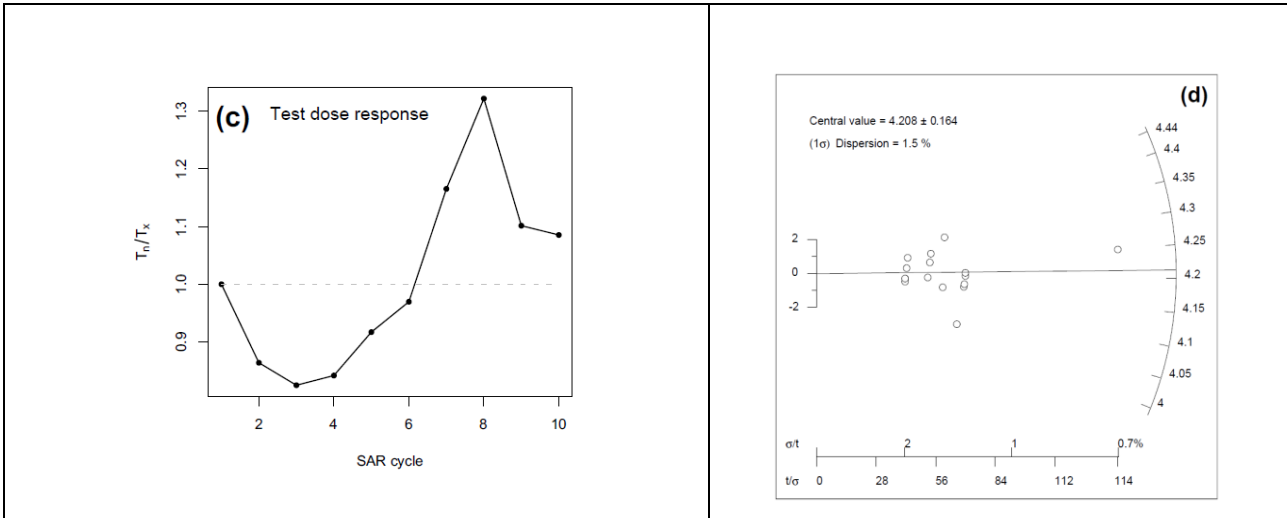


Figure. 8 Fast component quartz improved SAR analyses of the STRN-2 sample: the same comparative ED analyses were done for both samples. (a) Dose response curve fitting with exponential function (b) Monte Carlo simulation analyses of estimated ED point, obtained from Analyst.exe software (c) Test dose (1 Gy) response throughout SAR Cycle (d) Radial distribution of EDs, yielding ~4.2 Gy determined from 16 aliquots

7. DISCUSSION AND CONCLUSIONS

A multi-analytical tools that combine optical microscopy, XRD, XRF, TL and OSL techniques were successfully utilized in order to answer the main question of this paper: When was the last time that Erikli Basilica was used in Strotonikeia? The dating of brick samples was determined by using luminescence techniques. In this study, TL and OSL techniques have been used to find out the equivalent dose. The results of the obtained ages were represented at Fig.9, indicating that MAAD protocols using both thermally and optically stimulation types are in agreement with each other. In addition that, OSL ages of the sediments (STRN-2 and STRN-3) were indicated with blue and arrow, yielding about

1100 years. The ages of STRN-1, STRN-2 and STRN-3 support the claim that the coin should be attributed to the 10<sup>th</sup> century, which, in turn, shows until when the basilica was used. In classical SAR procedure for polymineral samples, IRSL sensitivity of discs was changed due to the repeated irradiation, preheating and measurement of the discs, which might be underestimation on determined doses as indicated in the literature (Duller et al., 1999; McKeever, 2001). Therefore, the ED results obtained from classical SAR procedure were ignored while determining, bringing about problematic results on luminescence ages. On the other hand, OSL improved SAR results acquired from the fast component of quartz mineral are consistent with MAAD outcomes.

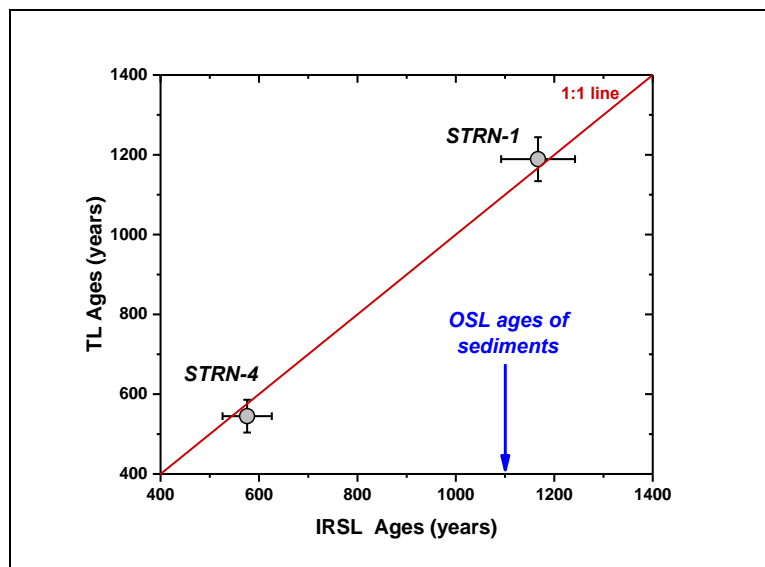


Figure. 9 Comparison of IRSL, OSL and TL ages from brick and sediment samples

The age of the STRN-4 (the sample from the wall) is found to be younger than the others (specimens from the floor), which indicates that the basilica's wall may have been repaired to be used for other purposes in some later date. Moreover, the wall (younger) and the floor (older) could have been built at different periods of site settlement. These results are supported by mineralogical components of the specimens.

Additionally, as a result of the mineralo-petrographic research, it is observed that the contents of the samples are different from each other. Based on this observation, it is highly probable that their materials were taken from different sand sources, since each source loses its productivity over time. New sources in different surrounding regions may be used in later periods. This and the other finding involving dating research both indicate that

the two samples might be produced in different time periods. This research is an interdisciplinary work to solve an archaeological problem with the help of natural science. We conclude that results obtained in our study may benefit the works in dating as well as support archaeological works in this region of Stratonikeia.

Although a small number of samples were elaborately studied, it is considerable that the first experimental report is presented from this archaeological site. Therefore, we believe that this study might shed light on the future knowledge of archaeological studies of the region. Comparing the outcomes, further dating studies using various methods, archaeological observations and characterization studies are required to get more precise conclusions about Stratonikeia archaeological site.

## ACKNOWLEDGEMENTS

This study was financially supported by Scientific Research Projects Unit of the Pamukkale University under grant number BAP-2012BSP028 and 2017KRM002-084. The authors would like to extend their special thanks to Prof. Dr. Bilal Söğüt (Department of Archeology, Pamukkale University), who is the director of the Stratonikeia excavation, for his contribution in fieldwork. We are very grateful to Prof. Dr. Niyazi Meriç (Director of Institute of Nuclear Sciences, Ankara University) for giving permission to use facilities and Dr. Kıymet Deniz (YEBİM, Ankara University) for her help during analytical procedures. We also would like to thank three reviewers for their insightful comments on the initial version of the present manuscript.

## REFERENCES

- Adamiec, G., & Aitken, M. J. (1998). Dose-rate conversion factors: update. *Ancient TL*, 16(2), 37-50.
- Aitken, M.J. (1985) *Thermoluminescence Dating*. Academic Press, London.
- Aitken M.J. (2013) *An Introduction to Optical Dating*. Oxford University Press, Oxford.
- Ankjærgaard, C., Jain, M., Thomsen, K.J. and Murray, A.S. (2010) Optimising the separation of quartz and feldspar optically stimulated luminescence using pulsed excitation. *Radiation Measurements*, Vol. 45, pp. 778-785.
- Bahçeli, S., Güleç G., Erdoğan H. and Söğüt B. (2016) Micro-Raman and FT-IR Spectroscopic studies of ceramic shards excavated from ancient Stratonikeia City at Eskişehir Village in West-South Turkey. *Journal of Mol. Struc.*, Vol. 1106, pp. 316-21.
- Belfiore, C.M., Day, P.M., Hein, A., Kilikoglou, V., La Rosa, V., Mazzoleni, P. and Pezzino, A. (2007) Petrographic and chemical characterization of pottery production of the Late Minoan I kiln at Haghia Triada, Crete. *Archaeometry*, Vol. 49, No. 4, pp. 621-53.
- Bortolussi, C., Panzeri, L., Sibilina, E., Zoleo, A., Brustolon, M., Martini, M., Salvatori, S. and Usai D. (2013) Luminescence and Electron Paramagnetic Resonance Properties of Prehistoric Ceramics from Al-Khiday Excavation Site, Sudan. *Mediterranean Archaeology and Archaeometry*, Vol. 13, No. 3, pp. 81-92.
- Cardiano, P., Ioppolo, S., Stefano, C.D., Pettignano, A., Sergi, S. and Piraino, P. (2004) Study and characterization of the ancient bricks of monastery of 'San Filippo di Fragalá' in Frazzanò (Sicily). *Analytica Chimica Acta*, Vol. 519, pp. 103-11.
- Correcher, V. and Delgado, A. (1998) On the use of natural quartz as transfer dosimeter in retrospective dosimetry. *Radiation Measurement*, Vol. 29, pp. 411-414.
- Durcan, J. A., King, G. E., & Duller, G. A. (2015). DRAC: Dose Rate and Age Calculator for trapped charge dating. *Quaternary Geochronology*, 28, 54-61.
- Doğan, M. and Meriç, N. (2014) 650 nm Laser stimulated dating from Side Antique Theatre, Turkey. *Radiation Phys. and Chem.*, Vol. 96, pp. 60-68.
- Duller, G.A.T., Botter-Jensen, L. and Mejdahl, V. (1999) An Automated Iterative Procedure for Determining Palaeodoses Using the SARA Method. *Quaternary Geochron.*, Vol. 18, pp. 293-301.

- Duller, G.A.T. (2007). Assessing the error on equivalent dose estimates derived from single aliquot regenerative dose measurements. *Ancient TL* **25**: 15-24.
- Duller, G. A. T. (2015). The Analyst software package for luminescence data: overview and recent improvements. *Ancient TL*, *33*(1), 35-42.
- Güllü, B. and Kadioğlu, Y.K. (2017) Use of tourmaline as a potential petrogenetic indicator in the determination of host magma: CRS, XRD and PED-XRF methods. *Spectrochimica Acta Part A*, Vol. 183, pp. 68-74.
- Hanfmann, G.M.A. and Waldbaum, J.C. (1968) Two submycenaean vases and a tablet from Stratonikeia in Caria. *American Journal of Archaeology*, Vol. 72, pp. 51-56.
- Hill, D.V., Speakman, R.J. and Glascock M.D. (2004) Chemical and Mineralogical Characterization of Sasanian and Early Islamic Glazed Ceramics from the Deh Luran Plain, Southwestern Iran. *Archaeometry*, Vol. 46, No. 4, pp. 585-605.  
<http://stratonikeia.pau.edu.tr> (last access date 2017 April 13)
- Javanshah Z. (2018) Chemical and mineralogical analysis for provenancing of the bronze age pottery from Shahr-i-Sokhta, South Eastern Iran, *Scientific Culture*, Vol. 4, No 1, (2018), pp. 83-92
- Kadioğlu, Y.K., Üstündağ, Z., Deniz, K., Yenikaya, C. and Erdoğan Y. (2009) XRF and Raman Characterization of Antimonite. *Instr. Sci. and Tech.*, Vol. 37, pp. 683-696.
- Koralay, T. and Kılıncarslan, S. (2016) A Multi-Analytical Approach for Determining the Origin of the Marbles in Temple-A from Laodicea ad Lycum (Denizli-Western Anatolia, Turkey). *Journal of Cultural Heritage*, Vol. 17, pp. 42-52.
- Li, B. (2010) The relationship between thermal activation energy, infrared stimulated luminescence and anomalous fading of K-feldspars. *Radiation Measurements*, Vol. 45, pp. 757-763.
- Liritzis, I., Polymeris, S.G. and Zacharias, N. (2010) Surface Luminescence Dating Of 'Dragon Houses' And Armena Gate At Styra (Euboea, Greece). *Mediterranean Archaeology and Archaeometry*, Vol. 10, No. 3, pp. 65-81.
- Liritzis, I., Stamoulis, K., Papachristodoulou, C., & Ioannides, K. (2013a). A re-evaluation of radiation dose-rate conversion factors. *Mediterranean Archaeology and Archaeometry*, *13*(3), 1-15.
- Liritzis, I., Singhvi, A. K., Feathers, J. K., Wagner, G. A., Kadereit, A., Zacharias, N., & Li, S. H. (2013b). *Luminescence dating in archaeology, anthropology, and geoarchaeology: an overview*. Heidelberg, Germany: Springer.
- Liritzis, I. and Vafiadou, A. (2015) Surface luminescence dating of some Egyptian monuments. *Journal of Cultural Heritage*, Vol: 16, pp. 134-150.
- McKeever, S.W.S. (2001) Optically Stimulated Luminescence Dosimetry. *Nucl. Instr. Meth. Phys. Res. B*, Vol. 184, pp. 29-54.
- McKeever, S.W.S. (2011) Optically stimulated luminescence: A brief overview. *Radiation. Meas.* Vol. 46, pp. 1336-1341.
- Morra, V., De Bonis, A., Grifa, C., Langella, A., Cavaza, L. and Piovesan R. (2013) Minero-Petrographic Study of Cooking Ware and Pompeian Red Ware (Rosso Pompeiano) from Cuma (Southern Italy). *Archaeometry*, Vol. 55, No. 5, pp. 852-879.
- Murray, A.S., Roberts, R.G. and Wintle, A.G. (1998) Luminescence dating of quartz using an improved single-aliquot regenerative-dose protocol. *Radiation Meas.*, Vol. 29, pp. 503-515.
- Öke, G. and Yurdatan, E. (2000) Optically stimulated luminescence dating of pottery from Turkey. *Talanta*, Vol. 53, pp. 115-119.
- Reedy, C.L. (2008) *Thin-Section Petrography of Stone and Ceramic Cultural Materials*. Archetype Publications, London.
- Quinn, P.S. (2013) *Ceramic Petrography: The Interpretation of Archaeological Pottery & Related Artefacts in Thin Section*. Archaeopress, Oxford.
- Prescott, J.R. and Hutton, J.T., 1994. Cosmic ray contributions to dose rates for luminescence and ESR dating: large depths and long-term time variations. *Radiation Measurements* *23*, 497-500.
- Polymeris, G. S., & Kitis, G. (2011). IRSL dating of a deep water core from Pylos, Greece; comparison to Post IR Blue OSL and TL dating results. *Mediterranean Archaeology & Archaeometry*, *11*(2), 107-120.
- Thomsen, K. J., Murray, A. S., Jain, M. and Bøtter-Jensen, L. (2008) Laboratory fading rates of various luminescence signals from feldspar-rich sediment extracts. *Radiation Measurements*, Vol. 43, pp. 1474-1486.

- Sabtu, S.N., Mahat, R.H., Amin, Y.M., Price, D.M., Bradley, D.A. and Maah, M.J. (2015) Thermoluminescence dating analysis at the site of an ancient brick structure at Pengkalan Bujang, Malaysia. *Applied Radiation and Isotopes*, Vol. 105, pp. 182-187.
- Söğüt, B. and Yılmaz, B. (2012) Stratonikeia'dan üç terrakotta mask (Three Terracotta Masks from Stratonikeia). *Pamukkale Univ. Journal Soc. Sci. Inst.*, Vol. 12, pp. 1-7 (Turkish).
- Şahiner, E., Meriç, N., & Uygun, S. (2013). Luminescence (IRSL) dating of Yeni Rabat church in Artvin, Turkey. *Radiation Physics and Chemistry*, 86, 68-73.
- Şahiner, E., Meriç, N. and Polymeris, G. S. (2014a) Assessing the impact of IR stimulation at increasing temperatures to the OSL signal of contaminated quartz. *Radiation Measurements*, Vol. 68, pp. 14-22.
- Şahiner, E., & Meriç, N. (2014b). A trapezoid approach for the experimental total-to-peak efficiency curve used in the determination of true coincidence summing correction factors in a HPGe detector. *Radiation Physics and Chemistry*, 96, 50-55.
- Şahiner, E. (2015). TL/OSL and ESR Methods Used in Paleoseismology Studies: Kütahya-Simav and North Anatolian Fault Zone. PhD Thesis, Ankara University, (in Turkish).
- Şahiner, E., Meriç, N. and Polymeris, G. S. (2017a) Thermally assisted OSL application for equivalent dose estimation; comparison of multiple equivalent dose values as well as saturation levels determined by luminescence and ESR techniques for a sedimentary sample collected from a fault gouge. *Nuclear Instruments and Methods in Physics Research Section B*, Vol. 392, pp. 21-30.
- Şahiner, E., Kitis, G., Pagonis, V., Meriç, N. and Polymeris, G. S. (2017b) Tunnelling recombination in conventional, post-infrared and post-infrared multi-elevated temperature IRSL signals in microcline K-feldspar. *Journal of Luminescence*, Vol. 188, pp. 514-523.
- Tsakalos, E., Christodoulakis, J., & Charalambous, L. (2016). The Dose Rate Calculator (DRc) for Luminescence and ESR Dating—a Java Application for Dose Rate and Age Determination. *Archaeometry*, 58(2), 347-352.
- Velosa, A.L., Coroado, J., Veiga, M.R., and Rocha, F. (2007) Characterisation of Roman mortars from Conímbriga with respect to their repair. *Materials Characterization*, Vol. 58, pp. 1208-16.